

**substance: hematite ( $\alpha$ -Fe<sub>2</sub>O<sub>3</sub>)**

**property: transport properties in doped Fe<sub>2</sub>O<sub>3</sub>**

**resistivity (first column) and activation energy (second column) for doped sinters at RT**

$\rho$ [ $\Omega$ cm]:	6.5·10 <sup>5</sup>	$E_A$ [eV]:	0.728	undoped sample	74C
	1.0·10 <sup>0</sup>		0.164	Ti doped,	1 at%
	5.1·10 <sup>0</sup>		0.191		0.1
	2.7·10 <sup>3</sup>		0.558		0.01
	4.0·10 <sup>1</sup>		0.207	Nb doped,	1 at %
	1.2·10 <sup>2</sup>		0.451		0.1
	1.0·10 <sup>3</sup>		0.602		0.01
	2.7·10 <sup>7</sup>		0.814	Cr doped,	1 at %
	5.9·10 <sup>7</sup>		0.814		0.1
	20.0·10 <sup>7</sup>		0.814		0.01
	1.2·10 <sup>6</sup>		0.722	Mn	1 at %
	6.3·10 <sup>6</sup>		0.722		0.1
	28.0·10 <sup>6</sup>		0.722		0.01
	3.9·10 <sup>7</sup>		0.809	V doped,	1 at %
	8.1·10 <sup>7</sup>		0.809		0.1
	25.0·10 <sup>7</sup>		0.809		0.01

**Ti doping:** The Ti concentration and the carrier concentration determined from Seebeck data assuming the density of states in the valence band  $g_v = [\text{Fe}]$  and the kinetic term = 0 are very similar [54M]. Mobility found to be activated [54M] with a temperature dependent activation energy; at high  $T$ ,  $E_A = 0.1$  eV. Activation energy for conductivity is also a function of Ti concentration [65G]: Figs. 1, 2. Seebeck effect: Figs. 3; also [67D]. Electron drift mobility for ceramic sample 0.10(2) cm<sup>2</sup>/V s at 1000 K. Hall coefficient: quite anomalous with  $R_H > 0$ , for  $T \leq T_N$ . In the region 1000 K <  $T$  < 1100 K,  $\mu_H \approx 0.025$  cm<sup>2</sup>/V s (ceramic sample) [67D].

**Zr and Nb doping:** Figs. 4, 5. From the exhaustion region, the drift mobility at 1200 K is 0.1 cm<sup>2</sup>/V s for ceramic sample. Comparison of Seebeck and conductivity data (Fig. 6) shows that  $S$  and  $\log \rho$  do not track, a result interpreted in terms of impurity conduction [70B]. Hall coefficient data have been interpreted in terms of spin-disorder scattering in a narrow band, with  $m_n \approx 9.5 m_0$ .

**Ca doping:** conductivity: Fig. 7, Seebeck coefficient: Fig. 3, p-type behaviour.

**Mg doping:** conductivity: Fig. 8, Seebeck coefficient: Fig. 9, p-type behaviour. In the temperature range 450...900°C, for Mg doped ceramic samples [66G] containing 0.2 at% Mg:  $\mu_p \approx (262/T) \cdot \exp(-0.1[\text{eV}]/kT)$  [cm<sup>2</sup>/V s] ( $T$  in K), a result completely at variance with the data for pure material. The Mg content cannot be increased beyond this level owing to spinel formation, MgFe<sub>2</sub>O<sub>4</sub>.

## References:

- 51M Morin, F. J.: Phys. Rev. 83 (1951) 1005.
- 54M Morin, F. J.: Phys. Rev. 93 (1954) 1195.
- 62T Tannhauser, D. S.: J. Phys. Chem. Solids 23 (1962) 25.
- 65G Geiger, G. H., Wagner, J. B.: Trans. AIME 233 (1965) 2092.
- 66G Gardner, R. F. G., Moss, R. L., Tanner, D. W.: Br. J. Appl. Phys. 17 (1966) 55.
- 67D van Daal, H. J., Bosman, A. J.: Phys. Rev. 158 (1967) 740.
- 70B Bosman, A. J., van Daal, H. J.: Adv. Phys. 19 (1970) 1.
- 74C de Logan, D., Lonergan, G. A.: Solid State Commun. 15 (1974) 577.

**Fig. 1.**

$\text{Fe}_2\text{O}_3\text{:Ti}$ . Conductivity vs. (reciprocal) temperature for Ti doped ceramic specimens in air and argon [65G]. For argon:  $p_{\text{O}_2}$  = equilibrium with  $\text{Fe}_2\text{O}_3$  and  $\text{Fe}_3\text{O}_4$ . Short-dashed curve: pure  $\text{Fe}_2\text{O}_3$  from [51M].

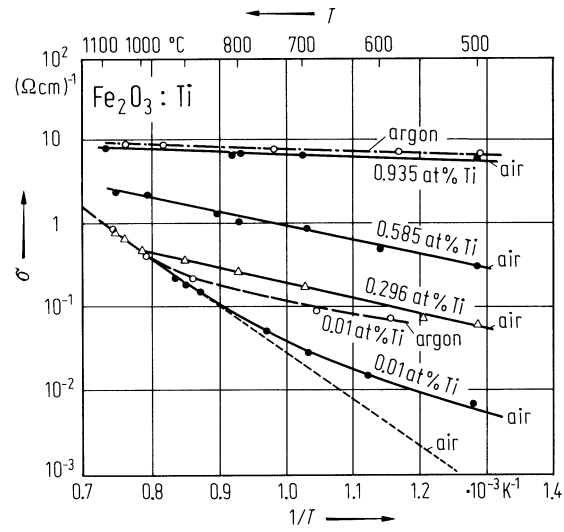


**Fig. 2.**

$\text{Fe}_2\text{O}_3:\text{Ti}$ . Activation energy for conductivity vs. Ti doping concentration in the temperature range where  $n_d$  ( $[\text{Ti}]$ ) is a constant [65G]. Ceramic sample.

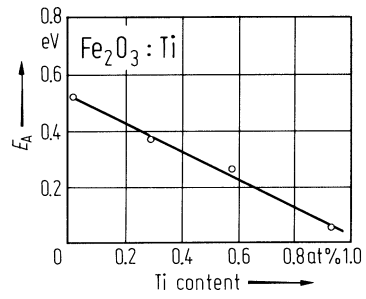


**Fig. 3.**

$\text{Fe}_2\text{O}_3:\text{Ti},\text{Ca}$ . Seebeck coefficient vs. temperature for Ti and Ca doped ceramic samples in air (open circles) and argon (full circles) ( $p_{\text{O}_2} \approx 10^{-4}$  atm) (\*: data from [62T]) [65G].

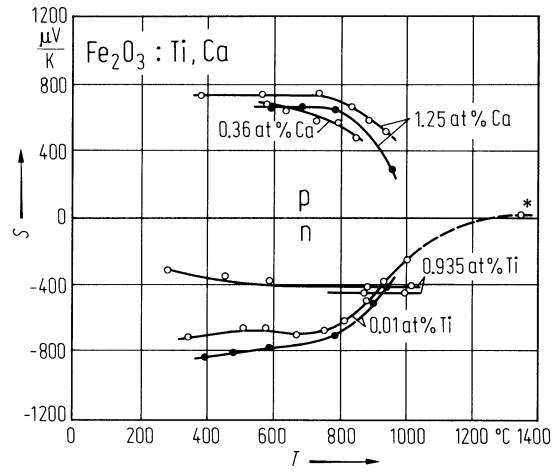


**Fig. 4.**

$\text{Fe}_2\text{O}_3\text{:Zr,Nb}$ . Seebeck coefficient, resistivity and Hall coefficient vs. (reciprocal) temperature for ceramic  $\alpha\text{-Fe}_2\text{O}_3$ . Open symbols in 0.01 atm  $\text{O}_2$ ; filled symbols in 1 atm  $\text{O}_2$ . Samples doped as follows: (1) 0.01 at% Zr, (2) 0.1 at% Zr, (3) 0.12 at% Nb, (4) 0.25 at% Nb, (5) 1 at% Zr [67D].

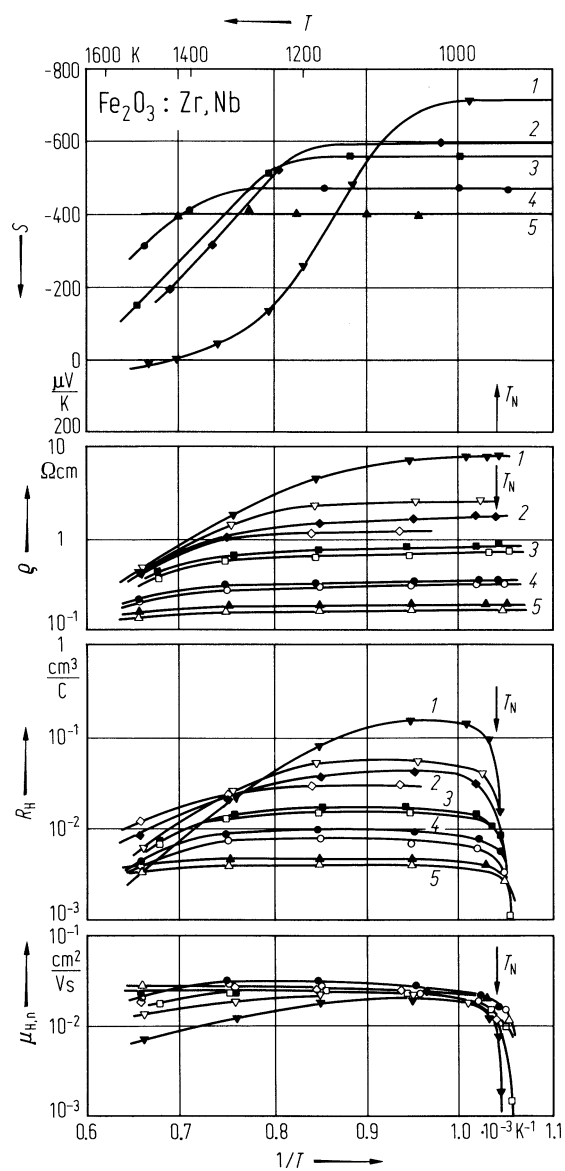


**Fig. 5.**

$\text{Fe}_2\text{O}_3\text{:Zr,Nb}$ . Resistivity vs. (reciprocal) temperature for Zr and Nb doped ceramic samples. Open symbols: dc results, filled symbols; ac results. Zr doped samples: (I) 0.01 at%, (2) 0.1 at%, (3) 0.25 at%, (4) 1.0 at%, Nb doped samples: (I,I') 0.1 at%, (II) 0.25 at%, (III) 0.5 at% [70B].

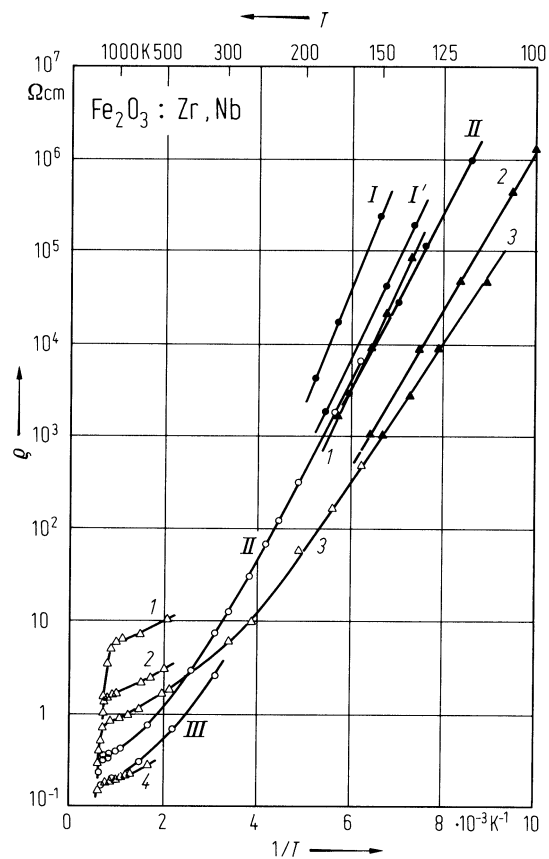


**Fig. 6.**

$\text{Fe}_2\text{O}_3\text{:Nb}$ . Resistivity and reduced Seebeck coefficient vs. (reciprocal) temperature for 0.1 at% Li doped p-type NiO, p-type CoO and p-type MnO and 0.1 at% Nb doped n-type  $\text{Fe}_2\text{O}_3$  [70B]. Ceramic samples.

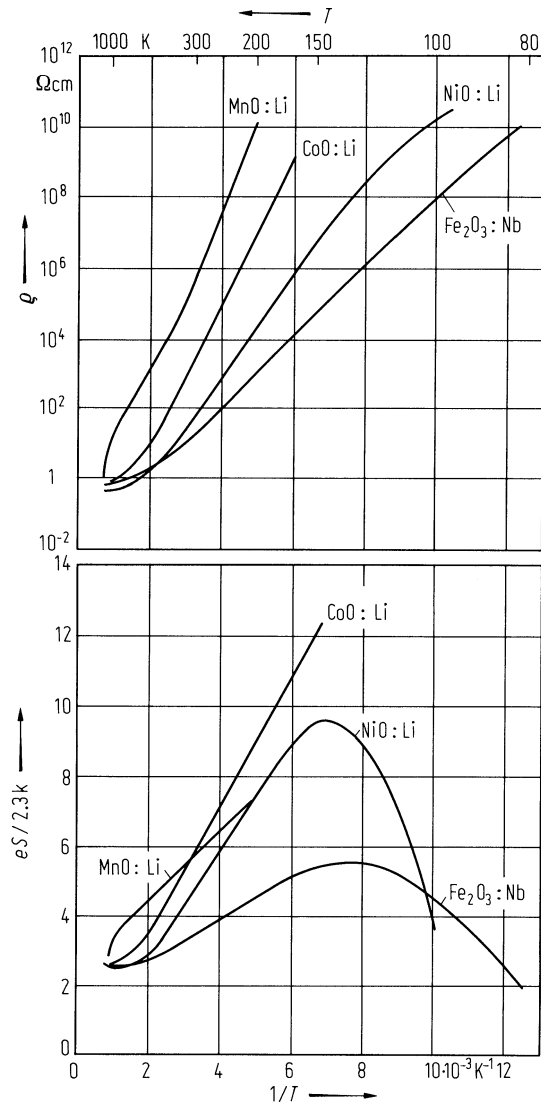




**Fig. 7.**

$\text{Fe}_2\text{O}_3:\text{Ti,Ca}$ . Conductivity vs. (reciprocal) temperature for 0.01 at% Ti doped  $\text{Fe}_2\text{O}_3$  (open circles), 0.30 at% Ca doped  $\text{Fe}_2\text{O}_3$  (full circles), in air (solid line), in argon (dashed line) ( $p_{\text{O}_2}$  in equilibrium with  $\text{Fe}_2\text{O}_3$  and  $\text{Fe}_3\text{O}_4$ ); *I*: data from [51M] on pure  $\text{Fe}_2\text{O}_3$ . [65G]. Ceramic samples.

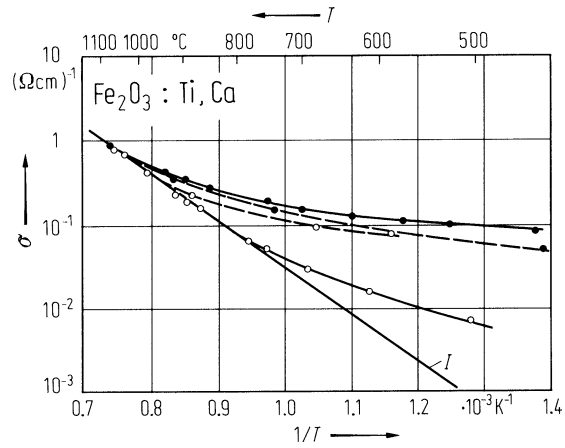


**Fig. 8.**

$\text{Fe}_2\text{O}_3:\text{Mg}$ . Conductivity vs. reciprocal temperature for Mg doped ceramic samples fired at 1300°C. (1) pure sample, (2) 0.01 at% Mg, (3) 0.03 at% Mg, (4) 0.05 at% Mg, (5) 0.2 at% Mg [66G].

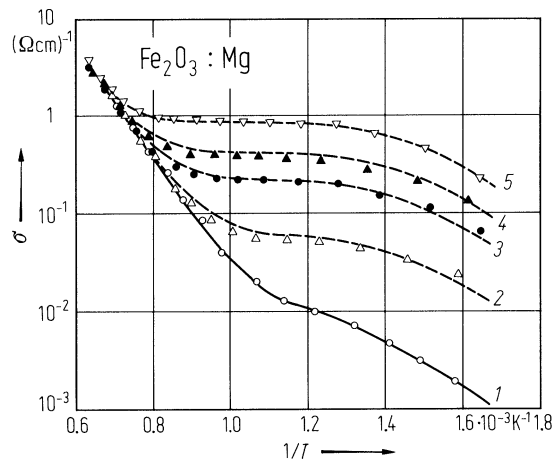


**Fig. 9.**

$\text{Fe}_2\text{O}_3\text{:Mg}$ . Seebeck coefficient vs. temperature. Samples as in Fig. 8 [66G].

